33rd Annual International Conference of the IEEE EMBS
Boston, Massachusetts USA, August 30 - September 3, 2011

# Adaptive Filtering for Suppression of Respiratory Artifact in Impedance Cardiography

Vinod K. Pandey, Prem C. Pandey, Nitin J. Burkule, and L. R. Subramanyan

*Abstract*— **Impedance cardiography is a noninvasive technique, based on sensing the variation in the electrical impedance of the thorax caused by variation in the blood volume during the cardiac cycle, for monitoring the stroke volume and some other cardiovascular indices. Respiratory and motion artifacts cause baseline drift in the sensed impedance waveform, particularly during or after exercise. This paper presents an LMS-based adaptive filtering technique for suppression of respiratory artifact for improving the estimation of the indices without smearing the beat-to-beat variations. It uses a reference signal, closely related to the respiratory artifact, obtained by a least-squares approximation based B-spline fitting on the contaminated impedance cardiogram in synchronism with the respiratory phases. The technique is evaluated on signals with simulated artifacts and on signals from nine healthy subjects and five patients with cardiovascular disorders. The values of the stroke volume, estimated on beat-to-beat basis, after suppression of respiratory artifact showed a good agreement with those from Doppler echocardiography.**

## I. Introduction

Impedance cardiography is a noninvasive technique for monitoring time varying impedance $Z(t)$ across the thorax due to blood flow. Negative derivative of $Z(t)$ is known as the impedance cardiogram (ICG). With the help of an appropriate impedance model of the thorax, it can be used for estimating the stroke volume (SV) and several other cardiovascular indices [1]−[3]. Fig.1 shows a typical ICG waveform. The ICG waveform has four main characteristic points: B, C, X, and O. Points B and X denote the aortic valve opening and closing, respectively. The point C corresponds to peak of the waveform. The point O indicates the time of opening of the mitral valve. The time interval between points B and X is the left ventricle ejection time ($T_{lvet}$). The stroke volume is generally calculated using Kubicek's formula or one of its several modifications [1]−[3] using two parameters: the left ventricular ejection time and the peak value of the ICG.

The sensed variation in the thoracic impedance is influenced by respiratory and motion artifacts [5]−[16]. Respiratory artifact is caused primarily by changes in the thoracic cage during the inhale and exhale phases of respiration, while motion artifact is related to the body movements. The spectra of these artifacts partly overlap with those of the ICG. The impedance variation caused by cardiovascular activity is typically $2-4\%$ of the basal impedance (usually about 20 $\Omega$), while the impedance variation caused by the artifacts may be up to 30% [3]. Thus the artifacts may cause a large baseline drift in the sensed waveform, resulting in errors in identification of the characteristic points and in the estimation of the stroke volume and other cardiovascular indices.

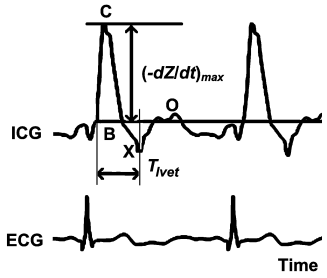


Fig. 1. A typical ICG along with ECG (adapted from [4]).

Holding the breath during recording can avoid respiratory artifacts, but it may change the stroke volume [6]. In the commonly used ensemble averaging technique, time frames in the ICG waveform are identified with reference to the R-peak of ECG and the parameters $T_{lvet}$ and $(-dZ/dt)_{max}$ are calculated from the ensemble averaged ICG [8]−[9]. It suppresses the non-coherent components related to the respiratory and motion artifacts, but it also suppresses beat-to-beat variations and transient changes in the signal. Because of heart rate variability, ensemble averaging tends to blur or suppress the less distinctive point B in the waveform. Further, beat-to-beat variation in the time interval between point B and R-peak may result in a smearing of the ICG peaks. Hurvitz *et al.* [9] used coherent ensemble averaging, by aligning B, C, and X points in each frame. The technique is free from the problems of beat-to-beat variation of cardiac events and event latency, but it can be applied only if the points can be reliably detected.

Several techniques have been reported for suppression of the artifacts from the ICG signal [10]−[16]. Barros *et al.* [15] used an adaptive filter with scaled Fourier linear combiner, with the ICG signal expressed as a scaled Fourier series with a period equal to the R-R interval. It may result in a distortion in the output waveform due to variation in time difference between the electrical and mechanical activities of the heart. Pandey and Pandey [16] used an adaptive filter, with the output of a thermistor based airflow sensor placed in front of the nostrils as the reference input, for

Manuscript received April 8, 2011; revised June 20, 2011.

V. K. Pandey was with the Indian Institute of Technology Bombay. He is now with the TCS Innovation Lab, Tata Consultancy Services, Thane, India (e-mail: vinod@ee.iitb.ac.in). P. C. Pandey is with the Department of Electrical Engineering, Indian Institute of Technology Bombay, Powai Mumbai 400 076, Maharashtra, India (corresponding author, tel.: +91-22-2576-7445, fax: +91-22-2572-3707, e-mail: pcpandey@ee.iitb.ac.in). N. J. Burkule was with the Asian Heart Institute and Research Center, Mumbai. He is now with the Jupiter Hospital, Thane, India (e-mail: burkule.nitin@gmail.com). L. R. Subramanyan is with the Department of Electrical Engineering, Indian Institute of Technology Bombay, India (e-mail: lrs@ee.iitb.ac.in).

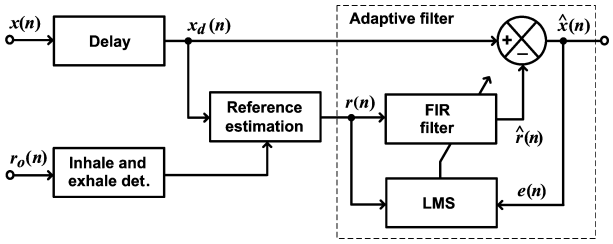


Fig. 2. Adaptive filtering technique using estimated respiration reference. $x(n)$ = sensed ICG signal (sum of the ICG $s(n)$ and the artifact $r_a(n)$), $r_o(n)$ = output of the respiration sensor, $\hat{x}(n)$= output signal.

LMS-based adaptive cancellation of the respiratory artifact from ICG signal. As the output of the respiration sensor is deficient in higher frequencies, the technique is not effective in suppressing higher spectral components of the respiratory artifact.

Unlike heart rate variability and blood pressure variability, stroke volume variability has not been widely used as a cardiac diagnostic tool, mainly because of the difficulty in getting accurate estimation of stroke volume on a beat-to-beat basis over a long period of time. This paper presents an LMS-based adaptive filtering technique for suppressing the respiratory artifact in the sensed thoracic impedance signal, without placing restrictions on breathing by the patient. The reference input for adaptive filtering is estimated using the output of a respiration sensor and the sensed impedance signal. A quantitative evaluation is carried out by applying the technique on signals with simulated artifacts at different signal-to-artifact ratios, for 23 healthy volunteers. A validation in a clinical setting is carried out for nine healthy subjects and five subjects with cardiovascular disorders, using Doppler echocardiography as a non-invasive reference technique for beat-to-beat estimation of the stroke volume.

## II. Signal Processing Technique

A schematic of the artifact suppression technique is shown in Fig. 2. The output signals from a thoracic impedance sensor and a respiration sensor are simultaneously acquired and used as the inputs to the adaptive filtering block for suppressing the respiratory artifact. Signal $x(n)$ is the sensed ICG. It is a sum of the desired signal $s(n)$ and the respiratory artifact $r_a(n)$, and is the primary input for adaptive filtering. The output of the respiration sensor $r_o(n)$, related to the respiratory artifact $r_a(n)$, is assumed to be uncorrelated to the signal $s(n)$. In our setup, a thermistor based airflow sensor, placed in front of the nostrils, senses the respiration. Its output $r_o(n)$ has a delay with respect to the artifact caused by the movement of the thoracic cage. A delay of $n_d$ samples, larger than the delay in the path of the sensed respiration, is introduced in the path of the primary signal $x(n)$. Number of taps in the adaptive filter is kept large enough to properly track the actual delay.

The output of the airflow sensor is synchronously related to the respiratory artifact, but it is found to be deficient in frequencies above about 1 Hz and hence it is not effective in suppressing higher spectral components of the respiratory artifact which severely affect the detection of the characteristic points in the ICG waveform. A signal closely related to the respiratory artifact can be estimated by using the output of the respiration sensor and the sensed impedance signal together and used as the reference input for the LMS-based adaptive filtering. As the respiratory artifacts during inhale and exhale phases are different, the reference needs to be estimated in synchronism with the respiratory phases. The two phases are detected from the sensed respiration $r_o(n)$, by taking the change in the polarity of its slope as the onset of a new respiratory phase. The reference $r(n)$ is estimated by a least-squares approximation based cubic B-spline [17], [18] fitted on $x_d(n)$, using a set of data points with equal number of uniformly spaced samples in each phase and the time indices corresponding to the two end points of each respiratory phase forming the knot vector.

The reference input $r(n)$ is filtered with the $M$-tap FIR filter, with coefficients $w_n(k)$, resulting in the output

$$\hat{r}(n) = \sum_{k=0}^{M-1} w_n(k) r(n-k). \tag{1}$$

The FIR filter output $\hat{r}(n)$ is subtracted from the delayed input $x_d(n)$ to get the denoised output

$$\hat{x}(n) = x(n-n_d) - \hat{r}(n). \tag{2}$$

The output $\hat{x}(n)$ is used as the error $e(n)$ for adaptive estimation of the filter coefficients by the LMS algorithm. It uses an instantaneous estimate of the gradient vector, based on sample values of the tap input vector and the error for dynamic adaptation to adjust filter coefficients on sample-by-sample basis [19], [20], using the equation

$$w_{n+1}(k) = w_n(k) + \mu\, e(n) r(n-k). \tag{3}$$

The step-size parameter $\mu$, satisfying the condition $0 < \mu < 2/M$(mean-square $(r(n))$, is selected for controlling the convergence and stability of the adaptation.

## III. Evaluation Method

The ICG signal was obtained from an ICG instrument developed at IIT Bombay [21], [22] using a four-electrode configuration [1] with disposable ECG spot electrodes. The signals acquired using this instrument and those using 'HIC-2000' (Bio-Impedance Technology, Inc., Chapel Hill, NC) exhibited similar artifacts [22]. The respiratory signal was sensed by placing a thermistor based respiration sensor ('SKRIPP-RRM-02', Pamtrons, Mumbai, India) close to the nostrils. Its position, in front of the nostrils, is not critical because the adaptive filtering adapts to the delay between the sensed respiration and the respiratory artifact. Waveforms of the ECG, basal impedance $Z_o$, thoracic impedance signal $Z(t)$, ICG, and respiratory signal were simultaneously acquired at a sampling frequency of 500 Hz using a 12-bit data acquisition unit ('KUSB-3102', Keithley, Cleveland, OH).

For a qualitative assessment, the technique was applied on signals from 52 healthy volunteers, recorded in pre-exercise and post-exercise relaxation conditions, with no restriction on breathing and the volunteer resting in a supine position in order to minimize motion artifact. The onsets of inhale

and exhale were detected using the sensed respiration. Least-squares approximation based cubic B-spline fitting on the contaminated input signal was carried out using the two end points of each respiratory phase as the knots. Use of 10 uniformly spaced samples in each respiratory phase as the data points resulted in a good approximation of the artifact. For quantifying the noise suppression, the technique was applied on signals with simulated respiratory artifact with different values of signal-to-artifact ratio generated using recordings from healthy volunteers. A validation of the technique was carried out on signals acquired in a clinical setting using Doppler echocardiography as a noninvasive reference technique.

### A. Suppression of Simulated Artifacts

A quantitative evaluation of the technique was carried out by processing signals generated as a weighted sum of artifact-free ICG and ICG-free artifact. Two types of signals were recorded from 23 healthy volunteers (age: $22-31$ years), with the volunteer resting in supine position without any non-ventilatory movements. During the first recording, the volunteer held the breath for 10 s. One of the cycles was repeatedly concatenated to obtain a periodic artifact-free ICG. During the second recording, the volunteer synchronized the inhale and exhale phases with $0.4$ Hz square wave displayed on an oscilloscope. Sixty cycles of the ICG were ensemble averaged with respect to the respiratory cycle to estimate one cycle of respiratory artifact. It was repeatedly concatenated to simulate a periodic ICG-free respiratory artifact.

The ICG-free artifact was scaled to have the same RMS value as the artifact-free ICG signal. The ICG-free artifact $r_o(n)$ was added to the artifact-free ICG $s(n)$ with a scaling factor $\alpha$ to obtain the contaminated ICG, with a signal-to-artifact ratio (SAR) of $-20\log\alpha$.

### B. Validation of the Technique under a Clinical Setting

For validating the technique for beat-to-beat estimation of the stroke volume under a clinical setting, Doppler echocardiography was used as the reference technique. Several studies have established a good correspondence between stroke volume estimated from Doppler echocardiography and other standard techniques [23], [24]. The signals from both the techniques were simultaneously acquired, at the Asian Heart Institute and Research Center, Mumbai, India. The investigation protocol was approved by the hospital's research committee and all the participating subjects read and signed an informed consent.

The signals were recorded from two groups of subjects: (a) 9 volunteers with normal health (male, $22-56$ years) and (b) 5 patients with cardiovascular disorders (male, $36-57$ years), excluding those with significant heart valve disease, pacemaker, myocardial infarction, and intra-cardiac shunts. Two sets of signals were recorded from each subject: (a) pre-exercise (with normal heart rate and respiration) and (b) post-exercise (with increased heart rate and respiration). The first set was recorded after the subject had rested for 15 min. The second set was recorded soon after the subject had performed a jogging exercise to increase the heart rate to 100 beat/min. The second set of signals was not recorded from two patients having difficulty in exercising. To avoid motion artifact related inaccuracies, both the sets of signals were recorded with the subject lying in the left lateral position.

Doppler echocardiograms were recorded, by a cardiologist, using ultrasonograph "GE Vivid 7 Dimension" in pulse-wave Doppler mode, in accordance with the recommendations in [25]. The ECG amplifier of the ultrasonograph was connected to three limb electrodes and a pulse output corresponding to the R-wave of the ECG was used for synchronizing the ICG and Doppler echocardiogram cycles.

Signals ECG, $Z_o$, $Z(t)$, ICG, respiration, and synchronization pulses were acquired along with the Doppler echocardiogram. The stroke volume was estimated using Kubicek's formula [1]−[3]

$$\mathrm{SV} = \rho\,(L/Z_o)^2(-dZ/dt)_{max}\,T_{lvet} \tag{4}$$

where, SV = stroke volume (mL), $\rho$ = blood resistivity (taken as 150 Ω-cm), $L$ = length between the sensing electrodes (cm), $Z_o$ = basal impedance (Ω), $(-dZ/dt)_{max}$ = maximum of the derivative of the impedance during the systole (Ω/s), and $T_{lvet}$ = left ventricular ejection time (s). Across the subjects, length between sensing electrodes, the basal impedance, and the impedance variation ranged $19.0-28.2$ cm, $17.0-39.0$ Ω, and $0.6-1.1$ Ω, respectively.

Estimation of $T_{lvet}$ requires a stable baseline. The value of $(-dZ/dt)_{max}$ is measured as the peak height from the point B or from the point of zero crossover. It is generally difficult to get a clear point B or a stable baseline in the waveform. An examination of the artifact-free signals, acquired from healthy volunteers during breath hold in the pre-exercise and the post-exercise conditions, showed that $(-dZ/dt)_{max}$ measured as the peak from the zero crossover point was approximately $0.72$ times the peak-to-peak height of $-dZ/dt$. This empirical relationship, also found to be valid in the clinical recordings not significantly contaminated by artifact, was used for estimating $(-dZ/dt)_{max}$. For estimating $T_{lvet}$, point B was taken as the notch near baseline crossover point and point X was taken as the most negative point in the cycle. The values of the left ventricular ejection time $(T_{lvet})$ and the stroke volume (SV) estimated using ICG were compared with those obtained by Doppler echocardiography.

## IV. Results

### A. Results for Suppression of Simulated Artifacts

The signals with simulated artifacts, of approximately 25 s duration and obtained as described in the previous section, were processed by adaptive filtering technique using estimated respiration reference (AFER). They were also processed by adaptive filtering using sensed respiration reference (AFSR) as reported earlier in [16]. Fig. 3 shows spectra of the ICG-free respiratory artifact, the sensed respiration, and the estimated respiration reference for a signal with 0 dB simulated artifact. The spectrum of the sensed respiration extends only up to about 1 Hz. However, the spectrum of

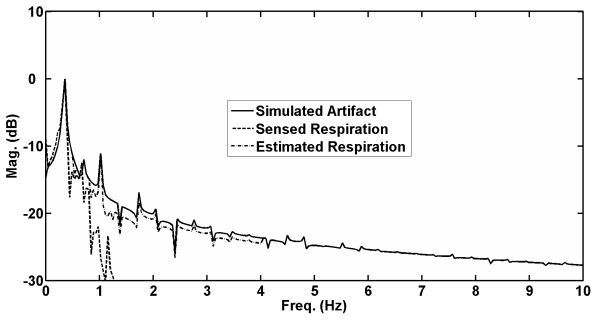


Fig. 3. Spectra of the ICG-free respiratory artifact, the sensed respiration, and the estimated respiration with controlled breathing at 0.4 Hz.

the estimated respiration closely approximates that of the ICG-free respiratory artifact, especially at higher frequencies. The same pattern was observed across all the signals with simulated artifacts. For AFSR, the most appropriate values of the processing parameters were sample delay $n_d \approx 270$, step-size $\mu \approx 2.1 \times 10^{-4}$ (for the reference inputs with RMS value of 0.25), and filter tap length $M \approx 400$. Corresponding values for AFER were $n_d \approx 270$, $\mu \approx 1.2 \times 10^{-4}$, and $M \approx 184$. The filter settling time were 5.0 s and 2.7 s for AFSR and AFER, respectively.

Application of the techniques on artifact-free signals resulted in the output signal-to-noise ratio of approximately 27.0 and 27.7 dB for AFSR and AFER, respectively, thus indicating no significant signal distortion. For the input SAR in the range of $-9$ dB to 9 dB, a plot of the output SAR versus the input SAR showed a nearly linear relationship, with the SAR increase of $18.2 - 18.8$ dB (mean = 18.5 dB) for AFSR and $19.3 - 19.8$ dB (mean = 19.6 dB) for AFER. Although AFER gave only 1.1 dB higher artifact attenuation, it was found to be very effective in improving the distinctness of the characteristic points. It needs a smaller filter tap length and adapts faster.

### *B. Results for Processing of Clinical Recordings*

Agreement between the values estimated from ICG and those from Doppler echocardiography was examined using three analyses: i) correlation (correlation coefficient), ii) linear regression (slope, offset error, and RMS error), iii) Bland-Altman test (mean bias, standard deviation of differences) [26]. These analyses were applied on beat-to-beat estimates from the signal recordings of 20 s duration (maximum permitted by the ultrasonograph), comprising $18 - 42$ cardiac cycles [22].

Fig. 4 shows a segment of the simultaneously recorded ECG, $Z(t)$, ICG, respiration, and synchronization pulse waveform, from a subject in post-exercise resting condition, and the corresponding segment of the processed ICG signal. It is difficult to locate the characteristic points in the ICG waveform due to the respiratory artifact. After processing, the artifact is reduced, facilitating the beat-to-beat localization of the characteristic points.

Across the recordings from the nine healthy subjects in the pre-exercise and the post exercise conditions, the heart rate

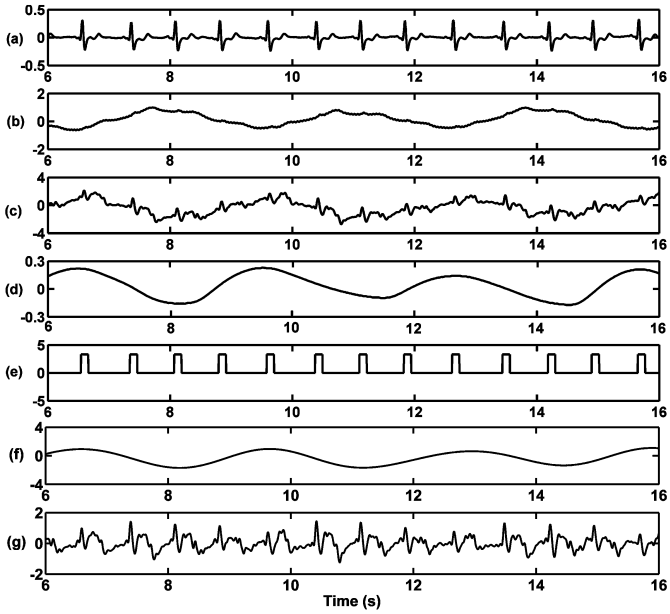


Fig. 4. Segment of waveforms for subject 'SH1' (age: 33 years, weight: 74 kg) in post-exercise relaxation: (a) ECG (in arbitrary units), (b) $Z(t)$ (in $\Omega$), (c) ICG (in $\Omega$/s), (d) sensed airflow (in arbitrary units), (e) synchronization pulse from Doppler echocardiograph (in V), (f) estimated reference, and (g) processed output (in $\Omega$/s).

and the breathing rate ranged $55 - 103$ beat/min and $10 - 25$ breath/min, respectively. The beat-to-beat values of $T_{lvet}$ and SV estimated by echocardiography ranged $204 - 385$ ms and $38 - 238$ mL, respectively, showing a large inter-cycle variability. The correlation coefficients for beat-to-beat estimation of SV from the unprocessed ICG ranged $0.15 - 0.80$, and they were statistically significant only in some of the cases. After processing, the corresponding values increased to $0.78 - 0.97$, and they were highly significant ($p < 0.001$) in all the cases. The processing resulted in best fit lines with slopes close to one. The RMS error from the best fit line decreased from $29.0 - 171.2$ mL to $5.8 - 42.8$ mL. The processing resulted in a decrease in the mean bias from $13.1 - 59.8$ mL to $1.2 - 11.2$ mL and a decrease in the standard deviation of the differences from $5.1 - 32.0$ mL to $1.5 - 8.3$ mL.

Across the recordings from the patients, the heart rate and the breathing rate ranged $62 - 114$ beat/min and $14 - 22$ breath/min, respectively. The beat-to-beat values of $T_{lvet}$ and SV estimated by echocardiography ranged $202 - 300$ ms and $32 - 78$ mL, respectively. The correlation coefficients for beat-to-beat estimation of SV from the unprocessed ICG ranged $0.20 - 0.64$ and none of the values were statistically significant. After processing, the values increased to $0.71 - 0.89$, and they were highly significant ($p < 0.0001$) in all the cases. Before processing, the slope of the best fit line varied from 0.6 to 1.9. After processing, the slope varied in a small range about 1. The RMS error from the best-fit line decreased from $38.3 - 146.3$ mL to $3.5 - 23.0$ mL. The mean bias decreased from $16.6 - 44.6$ mL to $0.3 - 10.9$ mL and the standard deviation of differences decreased from $7.5 - 23.9$ mL to $1.0 - 3.6$ mL.

## V. Discussion

Application of LMS-based adaptive filtering was investigated for suppressing the respiratory artifact, by estimating a reference by spline fitting on the ICG signal in synchronism with the respiratory phases detected from the output of a respiration sensor. While the spectra of the sensed respiration signal were deficient in spectral component above about 1 Hz, spectra of the estimated reference closely approximated the spectra of the respiratory artifact across the subjects. Use of estimated reference in place of sensed respiration significantly reduced the filter tap length and shortened the settling time to the duration of a typical respiratory cycle. It was found to be particularly effective in suppressing the artifacts in recordings with a large variation in the respiration rate and cardiac activity. The technique does not require identification of characteristic points and it is not affected by event variability.

Its application on artifact-free signals did not introduce any visible distortion. Processing of the signals with simulated respiratory artifact with input SAR in the range of $-9$ to 9 dB showed an SAR improvement of approximately 19.6 dB. Validation using recordings under a clinical setting showed that artifact suppression significantly improved the agreement of the SV values estimated on beat-to-beat basis from impedance cardiography to the corresponding values from Doppler echocardiography, in both the pre-exercise and the post-exercise conditions. The standard deviations of differences decreased to values comparable to the beat-to-beat variation in the stroke volume under pre-exercise condition and to values much smaller than the beat-to-beat variation in the post-exercise condition. In place of the LMS algorithm, other adaptation algorithms may be investigated for further shortening the settling time and improving the artifact suppression during high variability of respiration and cardiac activities. Effectivenss of the technique needs to be evaluated on the recordings from a larger number of patients with different cardiovascular disorders.

The morphology of artifact-free ICG may help in the diagnosis of cardiovascular disorders and it may be helpful in investigating methods for precise and accurate estimation of the stroke volume and other cardiovascular indices. It will facilitate study of beat-to-beat variation and the respiratory modulation of these indices.

## References


[1] W.G. Kubicek, F.J. Kottke, M.U. Ramos, R.P. Patterson, D.A. Witsor, J.W. Labree, W. Remole, T.E. Layman, H. Schoening, and J.T. Garamela, "The Minnesota impedance cardiograph - theory and application," *Biomed. Eng.*, vol. 9(9), pp 410-417, 1974.

[2] R.P. Patterson, "Fundamentals of impedance cardiography," *IEEE Eng. Med. Biol. Mag.*, vol. 8(1), pp 35-38, 1989.

[3] A. Sherwood, M.T. Allen, J. Fahrenberg, R.M. Kelsey, W.R. Lovallo, and L.J.P. van Doornen, "Methodological guidelines for impedance cardiography," *Psychophysiology*, vol. 27(1), pp 1-23, 1990.

[4] J. Malmivuo and R. Plonsey, *Bioelectromagnetism: Principles and Applications of Bioelectric and Biomagnetic Fields*. New York: Oxford University Press, 1995.

[5] Y. Zhang, M. Qu., J.G. Webster, W.J. Tompkins, B.A. Ward, and D.R. Bassett, "Cardiac output monitoring by impedance cardiography during treadmill exercise," *IEEE Trans. Biomed. Eng.*, vol. 33(11), pp 1037-1041, 1986.

[6] M.C. Du Quesnay, G.J. Stoute, and R.L. Hughson, "Cardiac output in exercise by impedance cardiography during breath holding and normal breathing," *J. Appl. Physiol.*, vol. 62(1), pp 101-107, 1987.

[7] Y. Miyamoto, T. Tamura, and T. Mikami, "Automatic determination of cardiac output using an impedance plethysmography," *Biotelemetry and Patient Monitoring*, vol. 8(4), pp 189-203, 1981.

[8] M. Muzi, T.J. Ebert, F.E. Tristani, D.C. Jeutter, J.A. Barney, and J.J. Smith, "Determination of cardiac output using ensemble-averaged impedance cardiograms," *J. Appl. Physiol.*, vol. 58(1), pp 200-205, 1985.

[9] B.E. Hurwitz, L.Y. Shyu, S.P. Reddy, N. Schneiderman, and J.H. Nagel, "Coherent ensemble averaging techniques for impedance cardiography," in *Proc. 3rd Annu. IEEE Symp. Comp. Based Med. Systems*, 1990, pp 228-235.

[10] Y. Yamamoto, M.S. Tamura, Y. Mouth, M. Miyasita, and H. Hamamoto, "Design and implementation for beat-by-beat impedance cardiography," *IEEE Trans. Biomed. Eng.*, vol. 35(12), pp 1086-1090, 1988.

[11] S.B. Raza, R.P. Patterson, and L. Wang, "Filtering respiration and low-frequency movement artefacts from the cardiogenic electrical impedance signal," *Med. Biol. Eng. Comput.*, vol. 30(5), pp 556-561, 1992.

[12] J. Ouyang, X. Gao, and Y. Zhang, "Wavelet-based method for reducing respiratory interference in thoracic electrical bioimpedance," in *Proc. 20th IEEE/ EMBC*, 1998, pp 1446-1449.

[13] V.K. Pandey and P.C. Pandey, "Wavelet based cancellation of respiratory artifacts in impedance cardiography," in *Proc. 15th Int. Conf. Digital Signal Processing*, Cardiff, U.K., 2007, pp 191-194.

[14] A. Krivoshei, V. Kukk, and M. Min, "Decomposition method of an electrical bio-impedance signal into cardiac and respiratory components," *Physiol. Meas.*, vol. 29(6), pp S15-25, 2008.

[15] A.K. Barros, M. Yoshizawa, and Y. Yasuda, "Filtering noncorrelated noise in impedance cardiography," *IEEE Trans. Biomed. Eng.*, vol. 42(3), pp 324-327, 1995.

[16] V.K. Pandey and P.C. Pandey, "Cancellation of respiratory artifact in impedance cardiography," in *Proc. 27th IEEE/ EMBC*, 2005, pp 3486-3489.

[17] C. De Boor, *A Practical Guide to Splines.* New York: Springer-Verlag, 1978.

[18] G. Farin, *Curves and Surfaces for CAGD: A Practical Guide.* San Diego: Academic, 2002.

[19] S. Haykin, *Adaptive Filter Theory.* New York: Pearson, 2005.

[20] S. Haykin and B. Widrow, *Least-mean-square Adaptive Filters.* New York: John Wiley, 2003.

[21] V.K. Pandey and P.C. Pandey, "Tracking-based baseline restoration circuit for acquisition of bio signals," *Electronics Letters*, vol. 43(6), pp 13-14, 2007.

[22] V.K. Pandey, "Suppression of artifacts in impedance cardiography," Ph.D. thesis, Dept. Biosciences and Bioengineering, Indian Institute of Technology Bombay, India, 2009.

[23] J. Christie, L.M. Sheldahl, F.E. Tristani, K.B. Sagar, M.J. Ptacin, and S. Wann, "Determination of stroke volume and cardiac output during exercise: comparison of two-dimensional and Doppler echocardiography, Fick oximetry, and thermodilution," *Circulation*, vol. 76(3), pp 539-547, 1987.

[24] A. Bouchard, S. Blumlein, N.B. Schiller, S. Schlitt, B.F. Byrd, T. Ports, and K. Chatterjee, "Measurement of left ventricular stroke volume using continuous wave Doppler echocardiography of the ascending aorta and M-mode echocardiography of the aortic valve," *J. Am. Coll. Cardiol.*, vol. 9(1), pp 75-83, 1987.

[25] M.A. Quiones, C.M. Otto, M. Stoddard, A. Waggoner, and W.A. Zoghbi, "Recommendations for quantification of Doppler echocardiography: a report from the Doppler Quantification Task Force of the Nomenclature and Standards Committee of the American Society of Echocardiography," *J. Am. Soc. Echocardiography*, vol. 15(2), pp 167-84, 2002.

[26] M.J. Bland and D.G. Altman, "Statistical methods for assessing agreement between two methods of clinical measurement," *Lancet*, vol. i, pp 307-310, 1986.